EUROPEAN ORGANISATION FOR NUCLEAR RESEARCH (CERN)

arXiv:1912.12198v2 [hep-ex] 2 Jan 2020

Search for an exotic S=-2, Q=-2 baryon resonance in proton-proton interactions at $\sqrt{s_{NN}}$ = 17.3 GeV

The NA61/SHINE Collaboration

Pentaquark states have been extensively investigated theoretically in the context of the constituent quark model. In this paper experimental searches in the $\Xi^- \pi^-$, $\Xi^- \pi^+$, $\overline{\Xi}^+ \pi^-$ and $\overline{\Xi}^+ \pi^+$ invariant mass spectra in proton-proton interactions at $\sqrt{s}$=17.3 GeV are presented. Previous possible evidence from the NA49 collaboration of the existence of a narrow $\Xi^- \pi^-$ baryon resonance in p+p interactions is not confirmed with almost 10 times greater event statistics. The search was performed using the NA61/SHINE detector which reuses the main components of the NA49 apparatus. No signal was observed with either the selection cuts of NA49 or a newly optimised set.

1 Introduction

During the past decades pentaquark states have been extensively investigated theoretically in the context of the constituent quark model [1, 2, 3, 4]. Some of these states are proposed to be closely bound and to have charge and strangeness quantum number combinations that cannot be realized as three-quark states. Using the chiral soliton model an anti-decouplet of baryons was predicted by Chemtob [5]. The lightest member was estimated by Praszalowicz [6] to lie at a mass of 1530 MeV. Diakonov et al. [7] subsequently derived a width of less than 15 MeV for this exotic baryon resonance, with $S = +1$, $J^P = \frac{1}{2}^+$. The mass and width of the experimentally observed Θ^+ [8] are close to the theoretical values, for review see Ref. [9]. Diakonov et al. [7] further made predictions for the heavier members of the anti-decouplet, with the isospin quartet of $S = -2$ baryons having a mass of about 2070 MeV and partial decay width into $\Xi\pi$ of about 40 MeV. This isospin $\frac{3}{2}$ multiplet contains two $\Xi_{3/2}$ with ordinary charge assignments $\left(\Xi_{3/2}^0, \Xi_{3/2}^-\right)$ in addition to the exotic states $\Xi_{3/2}^+$ ($uus s\bar{d}$) and $\Xi_{3/2}^{--}$ ($dds s\bar{u}$). The $\Xi_{3/2}$ isospin quartet has also been discussed as a part of higher multiplets. Jaffe and Wilczek [10] on the other hand base their predictions on the strong color-spin correlation force and suggest that the $\Theta^+(1540)$ baryon is a bound state of two highly correlated ud pairs and an antiquark. In their model the $\Theta^+(1540)$ has positive parity and lies in an almost ideally mixed $\overline{10}_f \oplus 8_f$ multiplet of $SU(3)_f$. For the isospin $\frac{3}{2}$ multiplet of Ξs they predict a mass around 1750 MeV and a width 50% greater than that of the $\Theta^+(1540)$.

Experimentally there is still a lack of consensus about whether the lightest member of the exotic anti-decouplet has been discovered. After almost fifteen years of excitement the results are inconclusive. There are also a number of reports from different groups that conducted searches for Θ^+ with some observing a signal and while others observing a null result, for review see Refs. [9, 11]. The reasons why some experiments see Θ^+, while the others do not, may be either of experimental nature or a peculiar production mechanism (or both).

The status of the heaviest members of the $\overline{10}$ multiplet that were seen only by the NA49 experiment at CERN [12] is even more problematic [13, 14]. This paper discusses the experimental search for the existence of the exotic $\Xi_{3/2}^{--}$ member of the Ξ multiplet essentially using the same detector with the same acceptance, similar analysis techniques, and in the same reaction as studied by the NA49 experiment, but with 10 times greater events statistics. The results of the search for the $\Xi_{3/2}^{--}$ and $\Xi_{3/2}^0$ states and their antiparticles in proton-proton interactions at $\sqrt{s} =17.3$ GeV are presented.

Recently the LHCb experiment at the LHC reported several high mass candidates for pentaquark states [15, 16] containig charm quarks and having masses above 4000 MeV, thus reviving the interest to this field.

2 The NA61/SHINE detector

Data used for the analysis reported here were recorded at the CERN SPS accelerator complex with the NA61/SHINE fixed target large acceptance hadron detector [17], which inherited most of the apparatus from NA49. The NA61/SHINE tracking system consists of 4 large volume time projection chambers (TPCs). Two of the TPCs (VTPC1 and VTPC2) are within superconducting dipole magnets. Downstream of the magnets two larger TPCs (MTPC-R and MTPC-L) provide acceptance at high momenta. The interactions were produced with a beam of 158 GeV/c protons on a cylindrical liquid hydrogen target of 20 cm length and 2 cm transverse diameter.
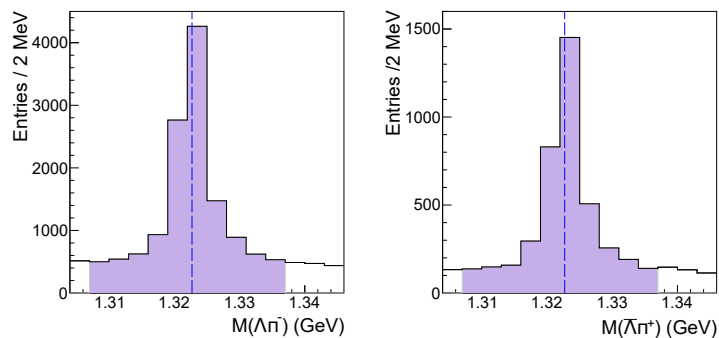
Figure 1: (Color online) The $\Lambda\pi^-$ invariant mass spectrum for Ξ^- candidates (*left panel*). Filled areas indicate the mass range of the selected candidates. The vertical dashed blue line shows the nominal PDG Ξ mass. Analogous $\bar{\Lambda}\pi^+$ invariant mass spectrum for $\bar{\Xi}^+$ candidates (*right panel*).

3 Analysis

The recorded data sample consists of about 53M events. Reconstruction started with pattern recognition, momentum fitting, and finally formation of global track candidates. These track candidates generally spanned multiple TPCs and consisted of charged particles produced in the primary interaction and at secondary vertices. The primary vertex was determined for each event. Events in which no primary vertex was found were rejected. To remove non-target interactions, the reconstructed primary vertex was required to lie within the target; ± 9 cm in the longitudinal (z) direction, and within ± 1 cm in the transverse (x, y) direction from the geometric center of the target. These cuts reduced the data sample to 33M inelastic and electromagnetic p+p interactions. Particle identification was performed via measurement of the specific energy loss (dE/dx) in the TPCs. The achieved resolution is 3–6% depending on the reconstructed track length [17, 18], and with extensive calibration. The dependence of the measured dE/dx on velocity was fitted to a Bethe-Bloch type parametrisation.

The first step in the analysis was the search for Λ candidates, which were then combined with the π^- to form the Ξ^- candidates. Next, the $\Xi^{--}_{3/2}$ $\left(\Xi^0_{3/2}\right)$ were searched for in the Ξ^- π^- (Ξ^- π^+) invariant mass spectrum, where the π^- (π^+) are primary vertex tracks. An analogous procedure was followed for the antiparticles.

Protons and pions were selected by requiring their dE/dx to be within 3σ around the nominal Bethe-Bloch value. The Λ candidates were identified by locating the vertices from neutral decays (so called V^0s, mostly upstream of VTPC1). To identify these V^0s, the protons were paired with π^- and both tracked backwards through the magnetic field. The V^0 was constrained to lie on the trajectory of the decay particle with the largest number of VTPC clusters. The V^0 position along the selected track and the three momentum components of both tracks (at that point) were found by a 4-parameter χ^2 fit.

Ξ^- candidates were assembled by the combination of all π^- with those Λ candidates having a reconstructed invariant mass within ± 15 MeV of the nominal PDG [19] mass. A fitting procedure is applied, using as parameters the decay position of the V^0 candidate, the momenta of both the V^0 decay tracks, the momentum of the daughter track, and finally the z position of the Ξ^- decay point. The x and y coordinates of the Ξ decay position are not subject to the minimization, as they are determined from the parameters using momentum conservation. This procedure yields the decay position and the momentum of the Ξ^- candidate.

Specific cuts were imposed to increase the significance of the Ξ^- signal. As the combinatorial background is concentrated close to the primary vertex, a distance cut of > 12 cm between the primary and the Ξ^- vertex was applied. Additional cuts on extrapolated track impact parameters in the x (magnetic bending) and y (non–bending) directions (b_x and b_y) at the primary vertex were imposed. To ensure that the Ξ^- originates from the primary vertex, its $|b_x|$ and $|b_y|$ were required to be less than 2 cm and 1 cm, respectively. On the other hand, the π^- from the Ξ^- decay were required to have $|b_y| > 0.2$ cm. The resulting $\Lambda\pi^-$ invariant mass spectrum is shown in Fig. 1 (*left*), where the Ξ^- peak is clearly visible. The Ξ^- candidates were selected within ± 15 MeV of the nominal Ξ^- mass. Only events with one Ξ^- candidate (95%) were retained. Exactly the same procedure was applied for antiparticles, resulting in the $\overline{\Xi}^+$ peak shown in Fig. 1 (*right*).
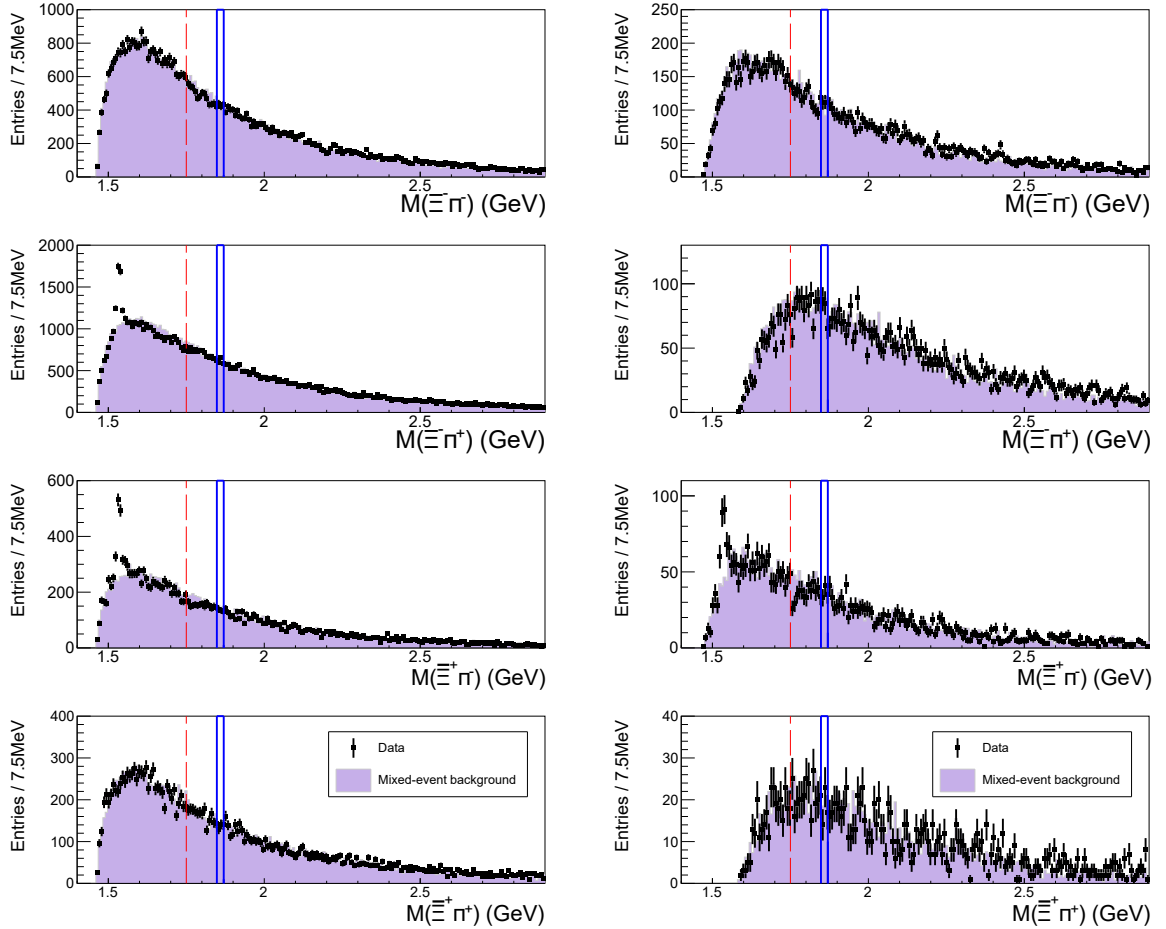

Figure 2: (Color online) Invariant mass spectra for $\Xi^- \pi^-$, $\Xi^- \pi^+$, $\overline{\Xi}^+ \pi^-$, $\overline{\Xi}^+ \pi^+$ after selection criteria optimized to maximize the signal to background ratio of the $\Xi(1530)$ (*left*) and after selection cuts following exactly the procedure of the NA49 experiment where possible evidence of the existence of $\Xi_{3/2}^{--}$ was found (*right*). The filled histograms are the normalised mixed-event background. The vertical dashed red line shows the theoretically predicted $\Xi_{3/2}^{--}$ mass [10]. The blue rectangle indicates the mass window in which the NA49 collaboration has seen an enhancement with significance up to 4.0 standard deviations. A narrow peak of the $\Xi(1530)^0$ state is observed in the invariant mass spectra of $\Xi^- \pi^+$ and of $\overline{\Xi}^+ \pi^-$.

To search for the exotic $\Xi_{3/2}^{--}$ the selected Ξ^- candidates were combined with primary π^- tracks. To select π^- from the primary vertex, their impact parameter $|b_y|$ was required to be less than 0.5 cm and their dE/dx

be within 2.5σ of their nominal Bethe-Bloch value. All cuts were optimized to maximize the signal-to-background ratio of the mass peaks of the $\Xi(1530)$, which decays into the same channel as the exotic pentaquark candidates. Moreover, to increase the signal-to-background ratio in the region of the $\Xi(1530)$, an additional $\theta > 1^o$ cut was applied, with θ being the opening angle between the Ξ^- and the π^- in the laboratory frame. All $\Xi\pi$ combinations were analysed following the same procedure. The resulting $\Xi^- \pi^-$, $\Xi^- \pi^+$, $\overline{\Xi}^+ \pi^-$ and $\overline{\Xi}^+ \pi^+$ invariant mass spectra are shown in Fig. 2 (*left*).

Additionally, a second set of more stringent selection criteria was implemented following exactly the procedure of the NA49 experiment in which possible evidence of the existence of the $\Xi_{3/2}^{--}$ was found [12]: the Ξ^- was required to have $|b_x| < 1.5$ cm and $|b_y| < 0.5$ cm at the primary vertex, the π^- from the Ξ^- decay $|b_y| > 0.5$ cm at the primary vertex, and the selected π^- from the primary vertex $|b_x| < 1.5$ cm and $|b_y| < 0.5$ cm. Moreover, the dE/dx had to be within 1.5σ of the nominal Bethe-Bloch value. The restriction on the opening angle between the Ξ^- and the π^- in the laboratory frame was $\theta > 4.5^o$. In addition to the described cuts, a lower cut of 3 GeV/c was imposed on the π^+ momenta to minimize proton contamination. The resulting $\Xi^- \pi^-$, $\Xi^- \pi^+$, $\overline{\Xi}^+ \pi^-$, and $\overline{\Xi}^+ \pi^+$ invariant mass spectra with NA49 selection criteria are shown in Fig. 2 (*right*).

4 Results

The invariant mass distributions of $\Xi^- \pi^-$, $\Xi^- \pi^+$, $\overline{\Xi}^+ \pi^-$, $\overline{\Xi}^+ \pi^+$ measured by NA61/SHINE are plotted in Fig. 2. The filled histograms show the mixed-event background normalised to the number of real combinations. The vertical dashed red line shows the theoretically predicted $\Xi_{3/2}^{--}$ mass. The blue rectangle indicates the mass window in which the NA49 collaboration has seen an enhancement with significance up to 4.0 standard deviations. For completeness, the sum of the four mass distributions is displayed in Fig. 3 for both sets of cuts. For the combined distributions NA49 reported a significance of 5.6 standard deviations. Independently of the implemented strategy of the signal-to-background optimization, the data is consistent with the mixed-event background in the mass window around the theoretical predictions of the $\Xi_{3/2}^{--}$ mass. No signal from $\Xi_{3/2}^{--}$, $\Xi_{3/2}^0$ states, and their antiparticles is observed in all invariant mass distributions.
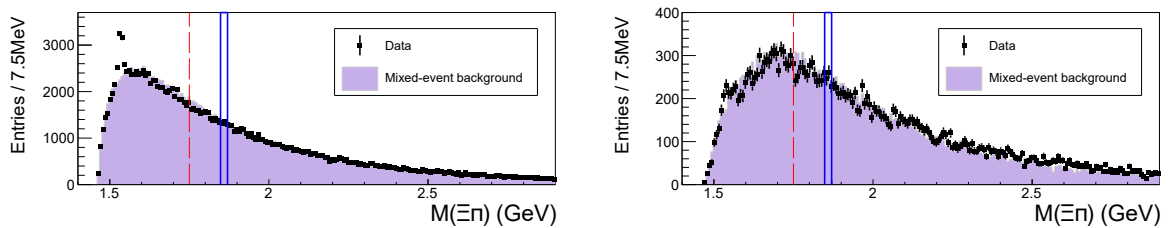

Figure 3: (Color online) The sum of the $\Xi^- \pi^-$, $\Xi^- \pi^+$, $\overline{\Xi}^+ \pi^-$, and $\overline{\Xi}^+ \pi^+$ invariant mass spectra after selection criteria optimized to maximize the signal-to-background ratio of the $\Xi(1530)$ (*left*), and after selection cuts following exactly the procedure of the NA49 experiment (*right*). The filled histograms are the normalised mixed-event background. The vertical dashed red line shows the theoretically predicted $\Xi_{3/2}^{--}$ mass [10]. The blue rectangle indicates the mass window in which the NA49 collaboration observed an enhancement with significance of 5.6 standard deviations. A narrow peak of the $\Xi(1530)^0$ state is observed.

The separate impact of the cuts was investigated by varying the dE/dx cut used for particle selection, by changing the width of accepted regions around the nominal Ξ^- and Λ masses, by investigating different

event topologies (e.g. the number of π mesons per event), by selecting tracks with different number of clusters, as well as by using different b_x and b_y cuts. Furthermore, the influence of resonances (including the possibility of particle misidentification) which could affect the signal was checked. In all cases no signal of $\Xi_{3/2}^{--}$ emerged.

Finally, a narrow peak of the $\Xi(1530)^0$ state is observed in the invariant mass spectra of $\Xi^- \pi^+$ for selection criteria optimized to maximize the signal to background ratio of the $\Xi(1530)$, and of $\overline{\Xi}^+ \pi^-$ for both selection criteria. The observed yield of the $\Xi(1530)^0$ scales appropriately with the number of events when comparing to NA49 results (using the NA49 selection criteria).

In conclusion, the NA61/SHINE analysis of p+p interactions with 10 times greater statistics do not confirm the NA49 indication of narrow $\Xi_{3/2}^{--}$, $\Xi_{3/2}^0$ states and their antiparticles. No signal is observed in all invariant mass distributions shown in Figs. 2 and 3. This is particularly true for the mass window (1848 - 1870 MeV) in which the NA49 collaboration had seen an enhancement with significance up to 5.6 standard deviations.

Acknowledgments

References

[1] M. Gell-Mann *Phys. Lett.* **8** (1964) 214–215.

[2] H. Hogaasen and P. Sorba *Nucl. Phys.* **B145** (1978) 119–140.

[3] D. Strottman *Phys. Rev.* **D20** (1979) 748–767.

[4] C. Roiesnel *Phys. Rev.* **D20** (1979) 1646.

[5] M. Chemtob *Nucl. Phys.* **B256** (1985) 600–608.

[6] M. Praszalowicz *Phys. Lett.* **B575** (2003) 234–241, `arXiv:hep-ph/0308114 [hep-ph]`.

[7] D. Diakonov, V. Petrov, and M. V. Polyakov *Z. Phys.* **A359** (1997) 305–314, `arXiv:hep-ph/9703373 [hep-ph]`.

[8] T. Nakano *et al.*, [LEPS Collab.] *Phys. Rev. Lett.* **91** (2003) 012002, `arXiv:hep-ex/0301020 [hep-ex]`.

[9] T. Liu, Y. Mao, and B.-Q. Ma *Int. J. Mod. Phys.* **A29** no. 13, (2014) 1430020, `arXiv:1403.4455 [hep-ex]`.

[10] R. L. Jaffe and F. Wilczek *Phys. Rev. Lett.* **91** (2003) 232003, `arXiv:hep-ph/0307341 [hep-ph]`.

[11] K. H. Hicks *Prog. Part. Nucl. Phys.* **55** (2005) 647–676, `arXiv:hep-ex/0504027 [hep-ex]`.

[12] C. Alt *et al.*, [NA49 Collab.] *Phys. Rev. Lett.* **92** (2004) 042003, `arXiv:hep-ex/0310014 [hep-ex]`.

[13] K. T. Knoepfle, M. Zavertyaev, and T. Zivko, [HERA-B Collab.] *J. Phys.* **G30** (2004) S1363–S1366, `arXiv:hep-ex/0403020 [hep-ex]`.

[14] S. Chekanov *et al.*, [ZEUS Collab.] *Phys. Lett.* **B610** (2005) 212–224, `arXiv:hep-ex/0501069 [hep-ex]`.

[15] R. Aaij *et al.*, [LHCb Collab.] *Phys. Lett.* **B784** (2018) 101–111, `arXiv:1804.09617 [hep-ex]`.

[16] R. Aaij *et al.*, [LHCb Collab.] *Phys. Rev. Lett.* **122** no. 22, (2019) 222001, `arXiv:1904.03947 [hep-ex]`.

[17] N. Abgrall *et al.*, [NA61/SHINE Collab.] *JINST* **9** (2014) P06005, `arXiv:1401.4699 [physics.ins-det]`.

[18] A. Aduszkiewicz *et al.*, [NA61/SHINE Collab.] *Eur. Phys. J.* **C77** no. 10, (2017) 671, `arXiv:1705.02467 [nucl-ex]`.

[19] M. Tanabashi *et al.*, [Particle Data Group Collab.] *Phys. Rev. D* **98** (Aug, 2018) 030001. `https://link.aps.org/doi/10.1103/PhysRevD.98.030001`.

The NA61/SHINE Collaboration

A. Aduszkiewicz [15], E.V. Andronov [21], T. Antićić [3], V. Babkin [19], M. Baszczyk [13], S. Bhosale [10], A. Blondel [4,23], M. Bogomilov [2], A. Brandin [20], A. Bravar [23], W. Bryliński [17], J. Brzychczyk [12], M. Buryakov [19], O. Busygina [18], A. Bzdak [13], H. Cherif [6], M. Ćirković [22], M. Csanad [7], J. Cybowska [17], T. Czopowicz [9,17], A. Damyanova [23], N. Davis [10], M. Deliyergiyev [9], M. Deveaux [6], A. Dmitriev [19], W. Dominik [15], P. Dorosz [13], J. Dumarchez [4], R. Engel [5], G.A. Feofilov [21], L. Fields [24], Z. Fodor [7,16], A. Garibov [1], M. Gaździcki [6,9], O. Golosov [20], V. Golovatyuk [19], M. Golubeva [18], K. Grebieszkow [17], F. Guber [18], A. Haesler [23], S.N. Igolkin [21], S. Ilieva [2], A. Ivashkin [18], S.R. Johnson [25], K. Kadija [3], N. Kargin [20], E. Kashirin [20], M. Kiełbowicz [10], V.A. Kireyeu [19], V. Klochkov [6], V.I. Kolesnikov [19], D. Kolev [2], A. Korzenev [23], V.N. Kovalenko [21], S. Kowalski [14], M. Koziel [6], A. Krasnoperov [19], W. Kucewicz [13], M. Kuich [15], A. Kurepin [18], D. Larsen [12], A. László [7], T.V. Lazareva [21], M. Lewicki [16], K. Łojek [12], B. Łysakowski [14], V.V. Lyubushkin [19], M. Maćkowiak-Pawłowska [17], Z. Majka [12], B. Maksiak [11], A.I. Malakhov [19], A. Marcinek [10], A.D. Marino [25], K. Marton [7], H.-J. Mathes [5], T. Matulewicz [15], V. Matveev [19], G.L. Melkumov [19], A.O. Merzlaya [12], B. Messerly [26], Ł. Mik [13], S. Morozov [18,20], S. Mrówczyński [9], Y. Nagai [25], M. Naskręt [16], V. Ozvenchuk [10], V. Paolone [26], O. Petukhov [18], R. Płaneta [12], P. Podlaski [15], B.A. Popov [19,4], B. Porfy [7], M. Posiadała-Zezula [15], D.S. Prokhorova [21], D. Pszczel [11], S. Puławski [14], J. Puzović [22], M. Ravonel [23], R. Renfordt [6], D. Röhrich [8], E. Rondio [11], M. Roth [5], B.T. Rumberger [25], M. Rumyantsev [19], A. Rustamov [1,6], M. Rybczynski [9], A. Rybicki [10], A. Sadovsky [18], K. Schmidt [14], I. Selyuzhenkov [20], A.Yu. Seryakov [21], P. Seyboth [9], M. Słodkowski [17], P. Staszel [12], G. Stefanek [9], J. Stepaniak [11], M. Strikhanov [20], H. Ströbele [6], T. Šuša [3], A. Taranenko [20], A. Tefelska [17], D. Tefelski [17], V. Tereshchenko [19], A. Toia [6], R. Tsenov [2], L. Turko [16], R. Ulrich [5], M. Unger [5], F.F. Valiev [21], D. Veberič [5], V.V. Vechernin [21], A. Wickremasinghe [24,26], Z. Włodarczyk [9], O. Wyszyński [12], E.D. Zimmerman [25], and R. Zwaska [24]

[1] National Nuclear Research Center, Baku, Azerbaijan
[2] Faculty of Physics, University of Sofia, Sofia, Bulgaria
[3] Ruđer Bošković Institute, Zagreb, Croatia
[4] LPNHE, University of Paris VI and VII, Paris, France
[5] Karlsruhe Institute of Technology, Karlsruhe, Germany
[6] University of Frankfurt, Frankfurt, Germany
[7] Wigner Research Centre for Physics of the Hungarian Academy of Sciences, Budapest, Hungary
[8] University of Bergen, Bergen, Norway
[9] Jan Kochanowski University in Kielce, Poland
[10] Institute of Nuclear Physics, Polish Academy of Sciences, Cracow, Poland
[11] National Centre for Nuclear Research, Warsaw, Poland
[12] Jagiellonian University, Cracow, Poland
[13] AGH - University of Science and Technology, Cracow, Poland
[14] University of Silesia, Katowice, Poland
[15] University of Warsaw, Warsaw, Poland
[16] University of Wrocław, Wrocław, Poland
[17] Warsaw University of Technology, Warsaw, Poland
[18] Institute for Nuclear Research, Moscow, Russia
[19] Joint Institute for Nuclear Research, Dubna, Russia
[20] National Research Nuclear University (Moscow Engineering Physics Institute), Moscow, Russia
[21] St. Petersburg State University, St. Petersburg, Russia
[22] University of Belgrade, Belgrade, Serbia

[23] University of Geneva, Geneva, Switzerland
[24] Fermilab, Batavia, USA
[25] University of Colorado, Boulder, USA
[26] University of Pittsburgh, Pittsburgh, USA